Molecular Orientation of Poly-3-hexylthiophene at the Buried Interface with Fullerene

Dhritiman Bhattacharyya, Angelo Montenegro, Purnim Dhar, Muhammet Mammetkuliyev, Robert M. Pankow^{§†}, Moon Chul Jung[‡], Mark E. Thompson, Barry C. Thompson[§], Alexander V. Benderskii*

Department of Chemistry, §Loker Hydrocarbon Research Institute, University of Southern California, Los Angeles, California 90089-0482, USA

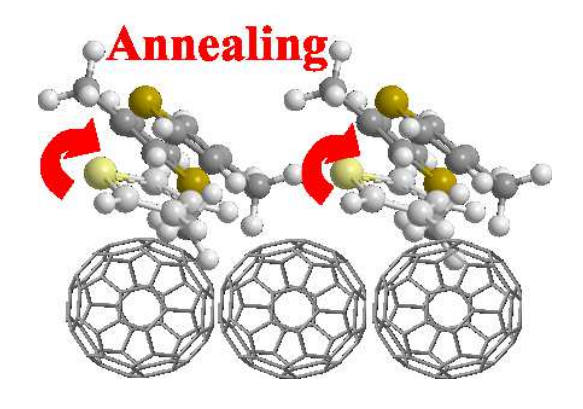
[†] These authors have contributed equally.

^{*} Corresponding author: <u>alex.benderskii@usc.edu</u>

Abstract

Molecular orientation at the donor-acceptor interface plays a crucial role in determining the efficiency of organic semiconductor materials. We have used vibrational sum frequency generation spectroscopy to determine the orientation of poly-3-hexylthiophene (P3HT) at the planar buried interface with fullerene (C_{60}). The thiophene rings of P3HT have been found to tilt significantly towards C_{60} , making an average angle $\theta \sim 49^0 \pm 10^0$ between the plane of the ring and the interface. Such tilt may be attributed to π - π stacking interactions between P3HT and C_{60} and may facilitate efficient charge transfer between donor and acceptor. Upon annealing, the thiophene rings tilt away from the interface by $\Delta\theta = (12-19)^0$. This may be attributed to higher crystallinity of annealed P3HT that propagates all the way to the interface, resulting in more 'edge-on' orientation, which is consistent with the observed red-shift by ~ 6 cm⁻¹ and spectral narrowing of the C=C stretch bands.

TOC graphic



The efficiency of an organic photovoltaic (OPV) device depends not only on the favorable alignment of the energy levels between the donor and the acceptor molecules, but also on the structure, morphology and the efficient packing of molecules in the active layer of a bulk heterojunction solar cell which control charge carrier generation and mobility. 1-6 Optimizing a solar cell material requires the optimization of every step that leads to the generation of electricity, including exciton dissociation, charge recombination and charge carrier mobility. The two competing processes, the exciton dissociation and the charge recombination, are guided by the orientation of the donor and the acceptor molecules at the interface and similarly the charge extraction processes and the contact resistance also depend on how molecules are oriented in contact with the electrode surfaces. 7-11 Nonadiabatic quantum molecular dynamics simulation by Mou et.al. 11 showed that a small change in molecular orientation at the interface can have a large effect on the charge transfer and the charge recombination rates in OPV materials. Several groups¹²⁻¹⁵ have separately studied electron donor and electron acceptor molecules at various dielectric surfaces by vibrational sum frequency generation (VSFG) spectroscopy. To the best of our knowledge, the orientation of electron donor molecules at the interface with an electron acceptor has not been reported. Knowledge of the orientation of the donor and acceptor moieties at the interface can help gain insight into the mechanisms of the exciton dissociation and charge recombination dynamics, and potentially make better devices by molecular design and material processing.4 Here, we focus on measuring the orientation of the backbone of poly-3hexylthiophene (P3HT) in contact with the fullerene surface.

High carrier mobility and high extinction coefficient in the visible range make P3HT an excellent donor material to be used in the active layer of organic photovoltaic devices and in organic field-effect transistors. ¹⁶⁻¹⁸ The thiophene rings of adjacent polymer chains are stacked

together through π - π interactions. ¹⁹⁻²¹ On the other side, fullerene and fullerene derivatives are well-known electron acceptor materials used in solar cells. The higher dielectric constant of fullerene (~ 4) compared to that of popular conjugated polymers (~ 3) makes it an ideal choice to facilitate exciton dissociation. ²² Also, high molecular symmetry of fullerene, which leads to triply degenerate LUMO levels ²³ and strong polarizability, also result in efficient charge mobility in this conjugated system. Thus, a P3HT-C₆₀ bilayer sample is a good model of the materials used in OPV devices.

To extract information about the molecular organization of the P3HT/C60 buried interface in a bilayer sample, we have used a surface selective non-linear spectroscopic technique, vibrational sum frequency generation (VSFG).²⁴⁻²⁷ VSFG is a second order nonlinear optical process which is electric dipole forbidden in a centrosymmetric environment, ²⁸ and hence does not have any contribution from the bulk phase of an isotropic material. In VSFG, a broadband tunable IR pulse is used to create vibrational coherence²⁹ of all the frequencies at the interface; a narrowband visible pulse is used to upconvert the coherences; and the sum frequency light is detected in the phase matching direction.²⁹⁻³¹ The VSFG spectrum is recorded for different polarizations of the input and the output beams and the change in VSFG signal intensity with polarization is exploited to obtain the molecular orientation of different functional groups at the interface.²⁶ For our experiment, we have used two different polarization combinations: PPP and SSP; where each combination denotes the polarization of the input IR light, input visible light and the output sum frequency light, from right to left. A detailed description of our experimental setup can be found in a previous publication³² and is also available in the Supporting Information (S.I.).

The VSFG selection rule dictates that for a vibrational mode to be SFG active, it must be both IR and Raman active. IR and Raman spectra (Fig.1) were collected for a P3HT/C₆₀ bilayer sample prepared by vapor-depositing 50 nm of C₆₀ on CaF₂ substrate and a P3HT film spin-coated from tetrahydrofuran solvent on top of it. We have made two different thicknesses of P3HT (60 and 25 nm) by changing the concentration of P3HT in the spin-coating solution, 11 mg/mL and 5.5 mg/mL. In the IR spectrum, the C-C inter-ring stretch, C=C symmetric and asymmetric stretch of the thiophene rings appear at 1380 cm⁻¹, 1410-1490 cm⁻¹ and 1510 cm⁻¹ respectively. In P3HT, there exists π - π conjugation between the thiophene monomers that extends up to 10-15 monomers or even more. 33-35 Different P3HT chains have different extents of such π conjugation, which leads to slightly different vibrational frequencies and hence inhomogeneous broadening in the IR and Raman spectra. The sharp feature at 1425 cm⁻¹ is due to the tangential mode of C₆₀ where the opposite pentagons contract and expand out of phase. 15,36 This feature is absent in the Raman spectrum. As previously reported by several groups, $^{37-39}$ the Raman spectrum of C_{60} shows a peak at 1469 cm⁻¹ assigned to the A_g pentagonal pinch mode. 14 This peak is not distinguishable in the Raman spectrum we recorded, as it is probably buried under the intense Raman peak originated due to C=C symmetric stretch of the thiophene ring.

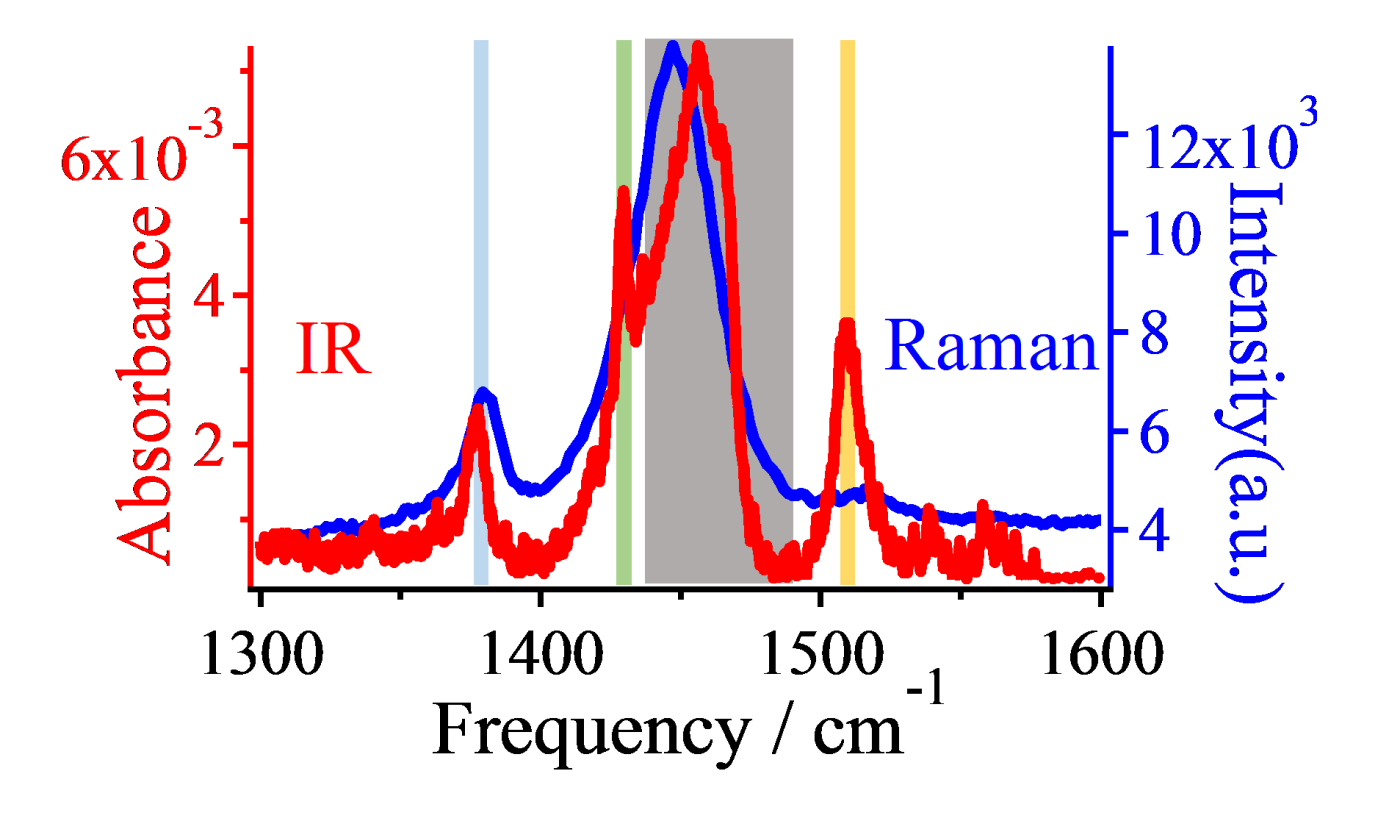


Figure 1. FTIR (red) and Raman (blue) spectra of P3HT/C₆₀ bilayer sample. The vibrational modes are shown using colored sticks: C-C inter ring stretch (faded blue line, 1380 cm⁻¹), C=C symmetric stretch modes (gray line, 1410-1490 cm⁻¹) and C=C asymmetric stretch (yellow line, 1510 cm⁻¹) of the thiophen ring. Vibrational mode of C₆₀ appears at 1425 cm⁻¹, shown by the green line.

After identifying the IR and Raman active modes of P3HT and C_{60} , polarization dependent VSFG experiments were performed to figure out the orientation of the P3HT backbone in contact with the fullerene surface. A previous publication by our group 12 showed that at P3HT/SiO₂ and P3HT/AlO_x, the majority of the SFG signal comes from the buried interface. Our Frensel factor calculation has also shown that the contribution of the C=C symmetric stretch of P3HT at P3HT/C₆₀ buried interface to the overall SFG intensity is ~100 times stronger than that of P3HT/air interface (Fig.S6, S.I.). As the P3HT/air interface contributes very little, in our current study we can safely assume that most of the collected SFG signal is coming from the P3HT/C₆₀ interface. The SFG spectra for P3HT/CaF₂ and P3HT/C₆₀/CaF₂ samples are shown in Figure 2. In both cases,

signals from PPP and SSP polarizations are shown. In the case of P3HT/CaF₂ samples, the SFG spectrum contains all three IR allowed vibrational modes as shown in Figure 2(a). In the region between 1430 to 1500 cm⁻¹, several SFG peaks are observed and all of them can be assigned to C=C symmetric stretch of the thiophene ring. The peak that appears at 1510 cm⁻¹ is due to the C=C asymmetric stretch. The SFG intensity for the PPP polarization shows higher intensity than that of SSP, in the C=C symmetric stretch region.

SFG spectra of 10 nm C₆₀ vapor-deposited on CaF₂ and SiO₂ substrates have been reported by Massari and co-workers. 14 Both IR active F_{1u} mode (1425 cm⁻¹) and Raman active A_g mode (1469 cm⁻¹) show SFG activity for C₆₀/CaF₂ sample. The relative intensity of these two peaks is different in our experiment as we have used a 50 nm film of C₆₀. Changing the thickness changes the interference between the signals coming from the top and the bottom interface of the C₆₀ film (Figure S1, S.I.). After identifying the peaks in the SFG spectrum of C₆₀, we move on to assign the spectra of the P3HT/C₆₀ bilayer sample (spin-coating solution of P3HT: 11 mg/mL in THF) which shows pronounced differences compared to P3HT/CaF₂. The SSP polarization shows higher intensity between 1430 to 1460 cm⁻¹; above that frequency, intensity for PPP polarization is higher. Also, the SSP spectrum shows a sharp peak at 1425 cm⁻¹ which is not present in P3HT/CaF₂. spectrum. This feature is coming from the SFG activity of the F_{1u} mode of fullerene. The SFG active peak of C₆₀ at 1469 cm⁻¹ is weak in intensity and probably buried under the SFG signal coming from the C=C symmetric stretch of P3HT. It is worth mentioning that in going from P3HT/CaF₂ sample to P3HT/C₆₀/CaF₂ sample, the signal intensity for SSP polarization increases by a factor of 3-4, whereas in PPP there is only a slight increase in intensity (Fig.2). Qualitatively, this points to the different orientation of P3HT in contact with C₆₀. Quantitative orientational analysis is presented below.

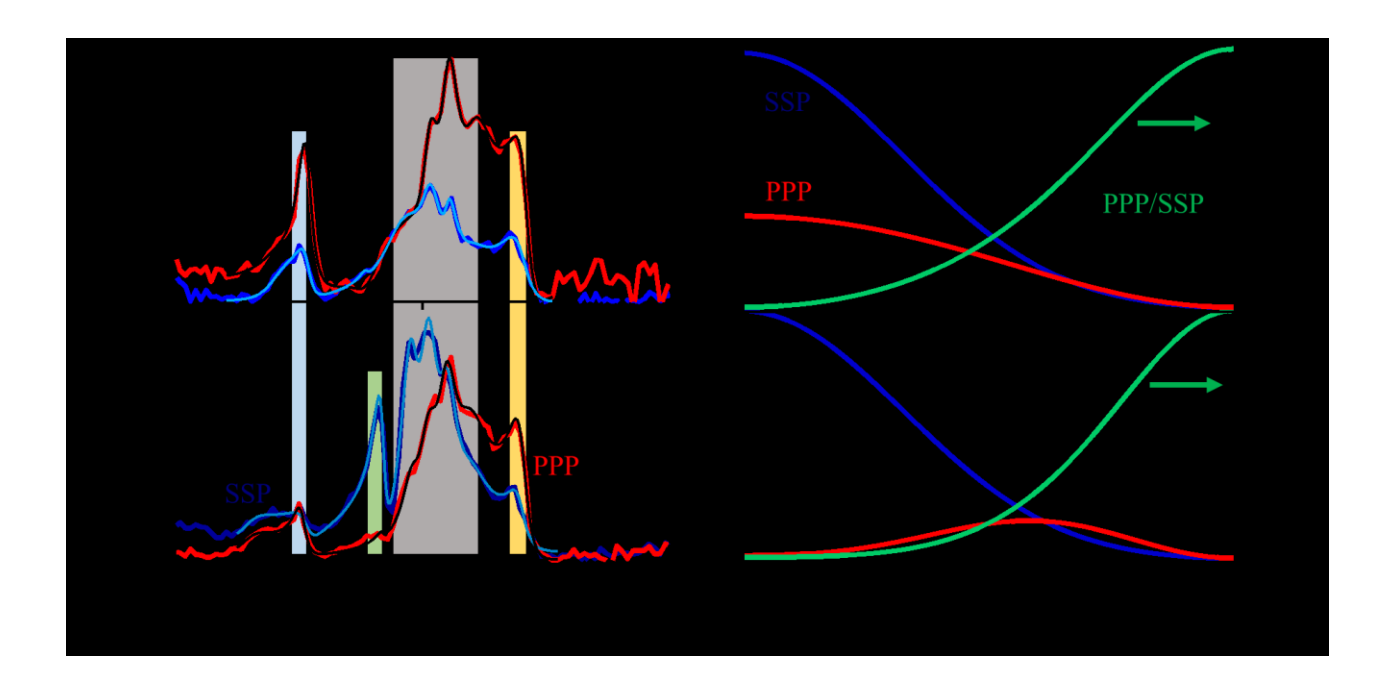


Figure 2. (a) SFG spectrum of P3HT spin-coated on CaF₂ substrate. Both PPP (red) and SSP (blue) spectra are shown. All IR active modes of P3HT appear in SFG spectrum as well: C-C inter ring stretch (faded blue line, 1380 cm⁻¹), C=C symmetric stretch (gray line, between 1430-1490 cm⁻¹) and C=C asymmetric stretch modes (yellow line, 1510 cm⁻¹) of the thiophene ring. (b) SFG spectrum of P3HT/C₆₀ bilayer sample. In addition to the peaks of P3HT, the sharp feature at 1425 cm⁻¹(green line) appears due to the IR active mode of C₆₀. (c) Calculated PPP (red), SSP (blue) SFG intensity and PPP/SSP intensity ratio (green) for P3HT/CaF₂ interface as a function of the tilt angle between the plane of the thiophene ring and the surface normal (d) Calculated plot for P3HT/C₆₀ interface.

According to the model proposed by Anglin et. al., 13 the adjacent thiophene rings of P3HT are connected with an average dihedral angle \angle S-C-C-S = 165 0 . As a result, for C=C symmetric stretch, the lateral component of the transition dipole of the neighboring thiophene rings gets canceled, while the out-of-plane components add up to give the net transition dipole orthogonal to the average plane of the ring pair, as shown in Figure 3(d). Hence, defining tilt angle θ between the net transition dipole with respect to the surface normal will help us extract orientation information about the P3HT backbone. θ =0 0 corresponds to "face-on" orientation of the thiophene rings, whereas θ =90 0 corresponds to "edge-on" orientation. For C=C symmetric stretch, only three

hyperpolarizability tensor elements contribute towards the VSFG spectra if C_{2v} symmetry is assumed for the thiophene ring. ²⁶ We also assume a Gaussian distribution of the tilt angle θ . ^{40,41} The calculated SFG intensity for PPP and SSP polarization along with the PPP/SSP intensity ratio are plotted as a function of the tilt angle for both P3HT/CaF₂ and P3HT/C₆₀ interface, as shown in Figure 2(c) and 2(d) respectively. The main uncertainty in this simulation comes from the unknown refractive index of the interfacial layer (n'). ^{26,31} As a result, while calculating the SFG intensity from an interface, n' is varied for IR, visible and sum frequency wavelengths; for P3HT/CaF₂ interface: 1.35<n'_{IR}<2.12; 1.43<n'_{VIS}<2.27; 1.43<n'_{SFG}<2.37; and for P3HT/C₆₀ interface: 1.97<n'_{IR}<2.12; 2.02<n'_{VIS}<2.27; 2.09<n'_{SFG}<2.37. We found out that PPP/SSP intensity ratio changes drastically with changing n'_{VIS} and n'_{SFG}; but it doesn't depend on n'_{IR}, as shown in the S.I. The confidence interval of '0' reported in this paper is estimated based on the assumed range of n'.

We have used eight Lorentzians to fit the SFG spectra for P3HT/CaF₂ and P3HT/C₆₀ samples. Two Lorentzians are used to fit the C-C inter-ring stretch region (1350-1400 cm⁻¹), five Lorentzians are used to fit the C=C symmetric stretch region (1400-1500 cm⁻¹) and one Lorentzian is used to fit the C=C asymmetric stretch which appears above 1500 cm⁻¹. As pointed out by other groups, ^{34,42} the C=C symmetric stretching mode of P3HT is very sensitive to the degree of molecular ordering which gives rise to the inhomogeneous broadening in the SFG spectra. Using five Lorentzians to fit the C=C symmetric stretch region will help us figure out how the orientation of the P3HT backbone changes depending on the extent of their molecular ordering. Comparing the experimental intensity ratio (PPP/SSP) to that of the theoretically calculated one, we find that there is a broad distribution of the orientation of the thiophene rings in contact with the CaF₂ surface. While most of the thiophene rings (in between 1450-1500 cm⁻¹) are stacked vertically

(edge-on) on CaF₂ substrate, thiophene rings with C=C symmetric stretch frequency below 1440 cm⁻¹ are significantly tilted towards the CaF₂ substrate making an average angle θ =42⁰ (33⁰ - 52⁰) between its transition dipole with respect to the surface normal. In contrast, at the P3HT/C₆₀ interface, all the thiophene rings, considering both long and short conjugation length polymer (the frequency of C=C symmetric stretch of thiophene ring red-shifts with increasing conjugation in the polymer), are tilted towards the C₆₀ moiety so that the net transition dipole of C=C symmetric stretch makes an average angle θ =49° from the surface normal with an orientational distribution between 38° and 64°. The orientation of different conformers of P3HT at the fullerene surface also depends on the processing condition of the P3HT film; for example, changing the spin-coating concentration of P3HT changes the orientation of different polymer chains by few degrees, as shown in Fig.S7. To investigate annealing induced structural change in P3HT/C₆₀ interface, the bilayer sample (P3HT spin-coating concentration 5.5 mg/mL) was annealed at 155°C for one hour. As shown in Figure 3(a) and 3(b); upon annealing, the SSP intensity decreases by ~45% between 1430–1500 cm⁻¹, whereas the PPP intensity increases by ~15% between 1430–1460 cm⁻¹ (gray shade) and decreases by ~45% between 1460-1500 cm⁻¹ (green shade), as compared to the unannealed sample. Fitting the annealed spectra and performing orientational analysis confirmed that the thiophene rings of P3HT, irrespective of long and short conjugation length, tilt back from the fullerene surface by 12^{0} - 19^{0} making an average angle of θ = 61^{0} between the net transition dipole and the surface normal.

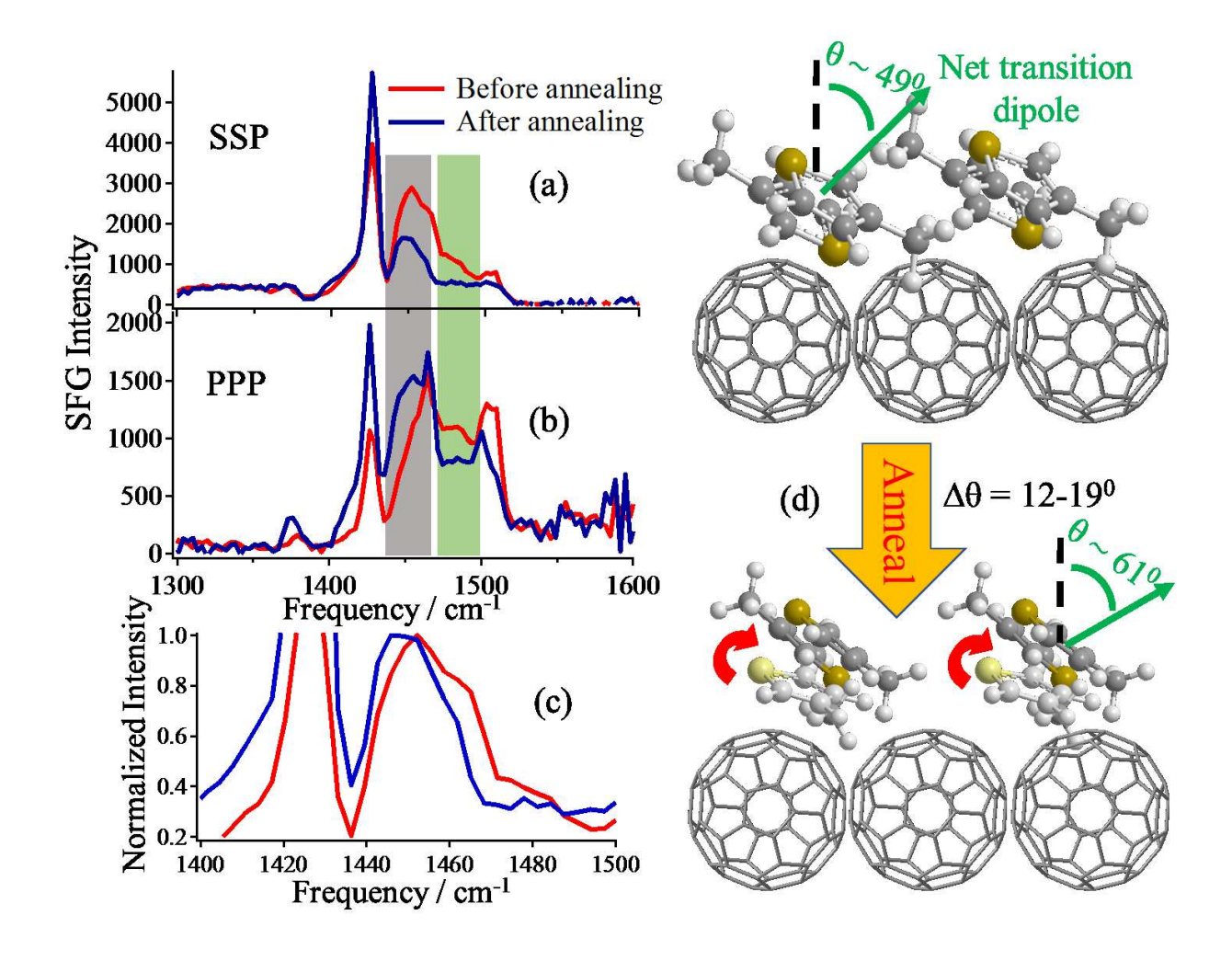


Figure 3. 3(a) and 3(b): Comparison of SFG spectrum of P3HT-C₆₀ bilayer sample before and after thermal annealing at 155^oC for one hour for SSP and PPP polarization respectively. (c) The normalized SSP spectra in the range 1430-1500 cm⁻¹ before (red) and after (blue) thermal annealing. (d) Cartoon figure of the orientation of P3HT at fullerene surface before and after annealing.

The SSP spectra before and after thermal annealing, normalized to intensity at 1450 cm⁻¹, are shown in Fig.3(c). Annealing results in a red shift of ~6 cm⁻¹, and narrower bandwidth. Different groups^{34,42-45} have used UV-VIS and Raman spectroscopy to show that thermal annealing leads to a higher degree of crystallinity (increasing molecular ordering) in P3HT. All those measurements were bulk-sensitive. There was no clear evidence so far that proves whether such

behavior occurs at the interface. The narrower spectral line and the red shift in the VSFG spectra of the annealed sample (Fig.3(c)) suggest that the effect of increased crystallinity in P3HT upon annealing propagates all the way to the interface. The effect of crystallinity is further corroborated by the increase in signal intensity of the characteristic C₆₀ peak at 1425 cm⁻¹ upon thermal annealing. This information may facilitate the use of annealing as a tool to tune the degree of molecular ordering and orientation of donor molecules at the interface with an electron acceptor.

We have demonstrated that interfacial orientation of the P3HT backbone depends on the nature of the underlying substrate. In contact with CaF₂ substrate, the thiophene rings tend to align themselves almost perpendicularly ('edge-on') to the plane of the substrate. At an interface with fullerene film, there is a significant tilt of the thiophene rings towards C₆₀ ('face-on'). Such tilt can be explained by the possibility of the π - π stacking between the thiophene rings and the conjugated C₆₀ molecules. This arrangement would be favorable for efficient charge transfer observed between electron donor (P3HT) and electron acceptor (C_{60}) molecule. ⁴⁶⁻⁴⁸ Upon thermal annealing, the thiophene backbone of P3HT tilts away from the surface of C_{60} by about $\Delta\theta$ =12±6 0 on average. adopting more edge-on orientation. This is accompanied by the higher degree of crystallinity of P3HT achieved upon thermal annealing, and the associated extending of the π conjugation over greater number of thiophene monomers in the P3HT chain, 34,42 as manifested by the red-shift and narrowing of the annealed spectra, indicating reduced inhomogeneous broadening. Annealing allows more efficient packing of the P3HT chains via π - π stacking interactions of neighboring P3HT molecules, which may overcome weaker interactions between P3HT and fullerene. Thus, upon annealing, the P3HT orientation at C₆₀ changes towards that at the weakly interacting CaF₂ interface (more 'edge-on'). Our results show that the molecular orientation at the donor-acceptor interface is the result of the interplay between donor-donor and donor-acceptor interactions, and

preparation conditions. The experimentally determined orientation of electron donor species in presence of electron acceptor can be used as a structural input to study the electron transfer processes theoretically. Understanding the role of donor-acceptor orientation towards efficient electron transfer may inform ways of improving photovoltaic efficiency.

Acknowledgments

This research was supported by AFOSR grant No. FA9550-15-1-0184. DB acknowledges support from the Burg Teaching Fellowship from Anton Burg Foundation. RMP acknowledges the Dornsife / Graduate School Fellowship and BCT acknowledges the NSF (CBET-1803063).

Supporting Information Available:

Experimental details, Spectral fitting parameters of SFG data, Plots of PPP/SSP ratio by changing non-linear hyperpolarizability (β) and refractive index (n), optical parameters for SFG orientational analysis.

References

- (1) Sirringhaus, H.; Brown, P. J.; Friend, R. H.; Nielsen, M. M.; Bechgaard, K.; Langeveld-Voss, B. M. W.; Spiering, A. J. H.; Janssen, R. A. J.; Meijer, E. W.; Herwig, P.; de Leeuw, D. M., Two-dimensional charge transport in self-organized, high-mobility conjugated polymers. *Nature* **1999**, *401*, 685-688.
- (2) Kline, R.J., McGehee, M.D. and Toney, M.F., Highly oriented crystals at the buried interface in polythiophene thin-film transistors. *Nat. Mater.* **2006**, *5*(3), 222-228.
- (3) Tada, A.; Geng, Y.; Nakamura, M.; Wei, Q.; Hashimoto, K., Interfacial modification of organic photovoltaic devices by molecular self-organization. *Phys. Chem. Chem. Phys.* **2012**, *14* (11), 3713-3724.
- (4) Beaujuge, P. M.; Fréchet, J. M. J., Molecular design and ordering effects in π -functional materials for transistor and solar cell applications. *J. Am. Chem. Soc.* **2011**, *133* (50), 20009-29.
- (5) Walter, S. R.; Youn, J.; Emery, J. D.; Kewalramani, S.; Hennek, J. W., In-situ probe of gate dielectric-semiconductor interfacial order in organic transistors: origin and control of large performance sensitivities. *J. Am. Chem. Soc.* **2012**, *134* (28), 11726–11733.
- (6) Horowitz, G., Organic thin film transistors: From theory to real devices. *J. Mater. Res.* **2004**, *19* (7), 1946-1962.
- (7) Brédas, J.L., Norton, J.E., Cornil, J. and Coropceanu, V., Molecular understanding of organic solar cells: the challenges. *Acc. Chem. Res.* **2009**, *42* (11), 1691-1699.

- (8) Holcombe, T.W., Norton, J.E., Rivnay, J., Woo, C.H., Goris, L., Piliego, C., Griffini, G., Sellinger, A., Bredas, J.L., Salleo, A. and Frechet, J.M., Steric control of the donor/acceptor interface: Implications in organic photovoltaic charge generation. *J. Am. Chem. Soc.* **2011**, *133* (*31*), 12106-12114.
- (9) Ratcliff, E.L., Zacher, B. and Armstrong, N.R., Selective interlayers and contacts in organic photovoltaic cells. *J. Phys. Chem. Lett.* **2011**, *2(11)*, 1337-1350.
- (10) Yi, Y., Coropceanu, V. and Brédas, J.L., Exciton-dissociation and charge-recombination processes in pentacene/C60 solar cells: theoretical insight into the impact of interface geometry. *J. Am. Chem. Soc.* **2009**, *131*(*43*), 15777-15783.
- (11) Mou, W., Ohmura, S., Shimojo, F. and Nakano, A., Molecular control of photoexcited charge transfer and recombination at a quaterthiophene/zinc oxide interface. *Appl. Phys. Lett.* 2012, *100*(20), 113.
- (12) Dhar, P.; Khlyabich, P. P.; Burkhart, B.; Roberts, S. T.; Malyk, S., Thompson, B.C. and Benderskii, A.V.; Annealing-Induced Changes in the Molecular Orientation of Poly-3-hexylthiophene at Buried Interfaces. *J. Phys. Chem. C* **2013**, *117* (29), 15213-15220.
- (13) Anglin, T.C., Speros, J.C. and Massari, A.M., Interfacial ring orientation in polythiophene field-effect transistors on functionalized dielectrics. *J. Phys. Chem. C* **2011**, *115*(32), 16027-16036.
- (14) Sohrabpour, Z.; Kearns, P. M.; Massari, A. M., Vibrational sum frequency generation spectroscopy of fullerene at dielectric interfaces. *J. Phys. Chem. C* **2016**, *120* (3), 1666-1672.
- (15) Silien, C.; Caudano, Y.; Longueville, J. L.; Bouzidi, S.; Wiame, F., HREELS, IR and SFG investigation of undoped and doped adsorbed fullerenes. *Surf. Sci.* **1999**, *s* 427–428 (99), 79-84.
- (16) Thompson, B. C.; Fréchet, J. M. J., Polymer-fullerene composite solar cells. *Angew. Chem., Int. Ed. Engl.* **2008**, *47* (1), 58-77.
- (17) Dodabalapur, A.; Laquindanum, J.; Katz, H. E.; Bao, Z., Complementary circuits with organic transistors. *Appl. Phys. Lett.* **1996**, *69* (27), 4227-4229.
- (18) Dang, M. T.; Hirsch, L.; Wantz, G., P3HT:PCBM, best seller in polymer photovoltaic research. *Advanced materials* **2011**, *23* (31), 3597-3602.
- (19) Prosa, T.J., Winokur, M.J., Moulton, J., Smith, P. and Heeger, A.J., X-ray structural studies of poly (3-alkylthiophenes): an example of an inverse comb. *Macromolecules* **1992**, *25*(17), 4364-4372.
- (20) Melis, C., Colombo, L. and Mattoni, A., Self-assembling of poly (3-hexylthiophene). *J. Phys. Chem. C* **2010**, *115*(2), 576-581.
- (21) Maillard, A. and Rochefort, A., Structural and electronic properties of poly (3-hexylthiophene) π -stacked crystals. *Phys. Rev. B* **2009**, *79*(11), 115207(1-7).
- (22) Mihailetchi, V. D.; Wildeman, J.; Blom, P. W. M., Space-charge limited photocurrent. *Phys. Rev. Lett.* **2005**, *94* (12), 126602(1-4).
- (23) Kanai, Y.; Grossman, J. C., Insights on interfacial charge transfer across P3HT/fullerene photovoltaic heterojunction from Ab initio calculations. *Nano Lett.* **2007**, *7* (7), 1967-72.
- (24) Chen, Z., Investigating buried polymer interfaces using sum frequency generation vibrational spectroscopy. *Prog. Polym. Sci.* **2010**, *35* (11), 1376-1402.
- (25) Chen, Z.; Shen, Y. R.; Somorjai, G. A., Studies of polymer surfaces by sum frequency generation vibrational spectroscopy. *Annu. Rev. Phys. Chem.* **2002**, *53*, 437-65.
- (26) Wang, H.F., Gan, W., Lu, R., Rao, Y. and Wu, B.H., Quantitative spectral and orientational analysis in surface sum frequency generation vibrational spectroscopy (SFG-VS). *Int. Rev. Phys. Chem.* **2005**, *24* (2), 191-256.
- (27) Gautam; Schwab; Dhinojwala; Zhang; Dougal; Yeganeh, Molecular structure of polystyrene at Air/Polymer and Solid/Polymer interfaces. *Phys. Rev. Lett.* **2000**, *85* (18), 3854-7.
- (28) Shen, Y.R., Surface properties probed by second-harmonic and sum-frequency generation. *Nature* **1989**, *337*(6207), 519-525.
- (29) Bordenyuk, A. N.; Jayathilake, H.; Benderskii, A. V., Coherent vibrational quantum beats as a probe of Langmuir-Blodgett monolayers. *J. Phys. Chem. B* **2005**, *109* (33), 15941-9.

- (30) Jayathilake, H. D.; Zhu, M. H.; Rosenblatt, C.; Bordenyuk, A. N.; Weeraman, C.; Benderskii, A. V., Rubbing-induced anisotropy of long alkyl side chains at polyimide surfaces. *J. Chem. Phys.* **2006**, *125* (6), 64706(1-9).
- (31) Zhuang, X.; Kim, D.; Miranda, P.; Shen, Y. R., Mapping Molecular Orientation and Conformation at Interfaces by Nonlinear Optics. *Phys. Rev. B* **1999**, *59*(19), 12632-12640.
- (32) Vinaykin, M.; Benderskii, A. V., Vibrational sum-frequency spectrum of the water bend at the air/water interface. *J. Phys. Chem. Lett.* **2012**, *3* (22), 3348-3352.
- (33) Beaujuge, P. M.; Amb, C. M.; Reynolds, J. R., Spectral engineering in π -conjugated polymers with intramolecular donor—acceptor interactions. *Acc. Chem. Res.* **2010**, *43* (11), 1396-1407.
- (34) Tsoi, W. C.; James, D. T.; Kim, J. S.; Nicholson, P. G.; Murphy, C. E.; Bradley, D. D.; Nelson, J.; Kim, J.-S., The nature of in-plane skeleton Raman modes of P3HT and their correlation to the degree of molecular order in P3HT: PCBM blend thin films. *J. Am. Chem. Soc.* **2011**, *133* (25), 9834-9843.
- (35) Park, M. S.; Aiyar, A.; Park, J. O.; Reichmanis, E.; Srinivasarao, M., Solvent evaporation induced liquid crystalline phase in poly (3-hexylthiophene). *J. Am. Chem. Soc.* **2011**, *133* (19), 7244-7247.
- (36) Weeks, D. E.; Harter, W. G., Vibrational frequencies and normal modes of buckminsterfullerene. *Chem. Phys. Lett.* **1988**, *144* (4), 366-372.
- (37) Yulong; Yijian; Jingqing; Yujun; Sishen; Zebo; Shengfa, Fundamental and higher-order Raman spectra of C60 films. *Phys. Rev. B: Condens. Matter Mater. Phys.* **1994,** *49* (7), 5058-5061.
- (38) Wang, X.Q., Wang, C.Z. and Ho, K.M., First-principles study of vibrational modes in icosahedral C 60. *Phys. Rev. B* **1993**, *48*(3), 1884-1887.
- (39) Bethune, D. S.; Meijer, G.; Tang, W. C.; Rosen, H. J.; Golden, W. G., Vibrational Raman and infrared spectra of chromatographically separated C 60 and C 70 fullerene clusters. *Chem. Phys. Lett.* **1991**, 179 (1-2), 181-186.
- (40) Simpson, G. J.; Rowlen, K. L., An SHG magic angle: dependence of second harmonic generation orientation measurements on the width of the orientation distribution. *J. Am. Chem. Soc.* **1999**, *121* (11), 2635-2636.
- (41) Wang, J.; Paszti, Z.; Even, M. A.; Chen, Z., Measuring polymer surface ordering differences in air and water by sum frequency generation vibrational spectroscopy. *J. Am. Chem. Soc.* **2002**, *124* (24), 7016-7023.
- (42) Gao, Y.; Grey, J. K., Resonance chemical imaging of polythiophene/fullerene photovoltaic thin films: mapping morphology-dependent aggregated and unaggregated $C \square C$ species. *J. Am. Chem. Soc.* **2009**, *131* (28), 9654-9662.
- (43) Verploegen, E.; Mondal, R.; Bettinger, C. J.; Sok, S.; Toney, M. F.; Bao, Z., Effects of thermal annealing upon the morphology of polymer–fullerene blends. *Adv. Funct. Mater.* **2010**, *20* (20), 3519-3529.
- (44) Li, G.; Shrotriya, V.; Huang, J.; Yao, Y.; Moriarty, T.; Emery, K.; Yang, Y., High-efficiency solution processable polymer photovoltaic cells by self-organization of polymer blends. In *Materials For Sustainable Energy: A Collection of Peer-Reviewed Research and Review Articles from Nature Publishing Group*, World Scientific: **2011**, pp 80-84.
- (45) Grigorian, S.; Joshi, S.; Pietsch, U. *Temperature-dependent structural properties of P3HT films*, IOP Conference Series: *Mater. Sci. Eng.* **2010**, 14(1), 012007.
- (46) Steim, R.; Kogler, F. R.; Brabec, C. J., Interface materials for organic solar cells. *J. Mater. Chem.* **2010**, *20* (13), 2499-2512.
- (47) Ma, H.; Yip, H. L.; Huang, F.; Jen, A. K. Y., Interface engineering for organic electronics. *Adv. Funct. Mater.* **2010**, *20* (9), 1371-1388.
- (48) Chen, L.-M.; Xu, Z.; Hong, Z.; Yang, Y., Interface investigation and engineering—achieving high performance polymer photovoltaic devices. *Journal of Materials Chemistry* **2010**, *20* (13), 2575-2598.